

# Structural basis for ligand-mediated mouse GITR activation

Zhaocai Zhou<sup>†</sup>, Yukiko Tone<sup>†</sup>, Xiaomin Song<sup>†</sup>, Keiji Furuuchi<sup>†</sup>, James D. Lear<sup>‡</sup>, Herman Waldmann<sup>§</sup>, Masahide Tone<sup>†¶</sup>, Mark I. Greene<sup>†¶</sup>, and Ramachandran Murali<sup>†¶</sup>

Departments of <sup>†</sup>Pathology and Laboratory Medicine and <sup>‡</sup>Biochemistry and Biophysics, University of Pennsylvania, Philadelphia, PA 19104; and <sup>§</sup>Sir William Dunn School of Pathology, University of Oxford, South Parks Road, Oxford OX1 3RE, United Kingdom

Communicated by Peter C. Nowell, University of Pennsylvania School of Medicine, Philadelphia, PA, November 27, 2007 (received for review October 4, 2007)

**Glucocorticoid-induced TNF receptor ligand (GITRL) is a member of the TNF super family (TNFSF). GITRL plays an important role in controlling regulatory T cells. The crystal structure of the mouse GITRL (mGITRL) was determined to 1.8-Å resolution. Contrary to the current paradigm that all ligands in the TNFSF are trimeric, mGITRL associates as dimer through a unique C terminus tethering arm. Analytical ultracentrifuge studies revealed that in solution, the recombinant mGITRL exists as monomers at low concentrations and as dimers at high concentrations. Biochemical studies confirmed that the mGITRL dimer is biologically active. Removal of the three terminal residues in the C terminus resulted in enhanced receptor-mediated NF- $\kappa$ B activation than by the wild-type receptor complex. However, deletion of the tethering C-terminus arm led to reduced activity. Our studies suggest that the mGITRL may undergo a dynamic population shift among different oligomeric forms via C terminus-mediated conformational changes. We hypothesize that specific oligomeric forms of GITRL may be used as a means to differentially control GITR receptor signaling in diverse cells.**

costimulation | oligomerization | regulatory | T cell | TNF

**G**lucocorticoid-induced TNF receptor (TNFR) family-related gene (*Gitr*) (*Tnfrsf18*) is a member of the TNFR super family (TNFRSF). The gene was first identified as a dexamethasone-inducible molecule on a murine T cell hybridoma (1). Its ligand, mouse glucocorticoid-induced TNF receptor ligand (m*Gitr*), was cloned by us, and the mechanism of its regulation was demonstrated (2). m*Gitr* expression is regulated by nuclear factor I (NFI), a key transcription factor, at low levels in nonstimulated B cells, macrophages, and bone marrow-derived dendritic cells (DCs), transiently up-regulated by LPS-stimulation, and then down-modulated (2, 3).

GITR is a type I transmembrane protein with homology to members of divergent costimulatory molecules in the TNFRSF (1, 4). To date three isoforms of GITR have been identified, including one soluble form that lacks a transmembrane domain (5). According to homology of the cytoplasmic domain, GITR and other three TNFRSF members (4-1BB, CD27, and OX40) probably constitute a new subfamily as divergent costimulators (6). GITR and the other subfamily members bind TRAF molecules and activate NF- $\kappa$ B (4, 7, 8).

GITR ligand (GITRL), a member of the TNF super family (TNFSF), is the natural ligand of GITR. Similar to all TNFSF members, GITRL is also a type II transmembrane protein with an extracellular C terminus and a short cytoplasmic segment. GITRL is one of the smallest (125 aa) in the TNFSF. GITRL is expressed on resting antigen-presenting cells (APCs), and its expression is transiently up-regulated and then down-regulated by triggering through BCR, CD40, or different Toll-like receptors (3). Mouse GITRL is not reported to exist as soluble ligand and likely functions as a membrane-bound molecule.

Crystallographic studies of TNFs and their cognate receptors revealed that ligand-mediated trimeric recruitment is the structural paradigm for the ligand-receptor signaling complexes of the entire

TNF/TNFR super family (9). OX40L and GITRL belong to the divergent subfamily of costimulatory molecules in the TNFSF (6), and they both have unusually short linker (6–7 residues versus an average of 50 for other TNFSF members) between the extracellular TNF homology domain and the transmembrane region (10). We have determined the crystal structure of mGITRL. We expected that mGITRL to form a trimer resembling the recently reported structure of OX40L (11). However, our results show that soluble mGITRL associates as a homodimer, which does not fit the paradigm. Biochemical studies demonstrate that the dimeric species is biologically active. Thus, dimeric GITRL may have a unique functional role in innate and adaptive immunity distinct from the biologically active trimeric GITRL in accordance with the structural paradigm of the TNFSF.

## Results

**Overall Structure of mGITRL.** The x-ray crystal structure of mGITRL was solved by the multiple isomorphous replacement method after repeated attempts to solve the structure by molecular replacement using the known TNFSF structures as search models failed. Crystals of mGITRL contain two molecules (designated as A and B) in the asymmetric unit. Structures of A and B are essentially identical with a root mean square deviation (rmsd) of 1.13 Å for 125 C $\alpha$  atoms. The overall structural core of the mGITRL monomer is conserved, showing a compact  $\beta$ -sandwich topology similar to the closely related OX40L (rmsd of 2.26 Å), albeit related with low sequence homology ( $\approx 13\%$ ) [supporting information (SI) Fig. 7]. However, several unique structural features of mGITRL monomer were clearly defined (Fig. 1*a*). First, the  $\beta$ -strand F that is part of the core  $\beta$ -sheet A'-A-H-C-F involved in oligomerization is split at the middle with a short fragment of loop inserted. Second, the interconnecting loops between the  $\beta$ -strands A and A', D and E, E and F were substantially shortened compared with the canonical TNFSF members. However, shortening of these loops did not lead to a lengthening of the subsequent  $\beta$ -strands B', B, C, D, E, F, G, and H. Third, the C terminus of mGITRL extends away from the core like an arm (residue Pro-167–Ser-173) (Fig. 1*a*). An extra  $\beta$ -strand (I) was formed at the very end of the C terminus arm. Notably, the C-terminus region is well defined in the electron density (Fig. 1*b*). This type of C-terminal disposition has not been observed in other TNFSF members. Moreover, the C terminus mediated a novel oligomeric form observed for TNFSF members (described below).

Author contributions: Z.Z. and Y.T. contributed equally to this work; M.T., M.I.G., and R.M. designed research; Z.Z., Y.T., X.S., K.F., J.D.L., M.T., and R.M. performed research; H.W., M.T., M.I.G., and R.M. analyzed data; and M.I.G. and R.M. wrote the paper.

The authors declare no conflict of interest.

Data deposition: The atomic coordinates and structure factors have been deposited in the Protein Data Bank, [www.pdb.org](http://www.pdb.org) (PDB ID code 2Q8O).

<sup>¶</sup>To whom correspondence may be addressed. E-mail: [mtone@mail.med.upenn.edu](mailto:mtone@mail.med.upenn.edu), [green@reo.med.upenn.edu](mailto:green@reo.med.upenn.edu), or [murali@xray.med.upenn.edu](mailto:murali@xray.med.upenn.edu).

This article contains supporting information online at [www.pnas.org/cgi/content/full/0711206105/DC1](http://www.pnas.org/cgi/content/full/0711206105/DC1).

© 2008 by The National Academy of Sciences of the USA

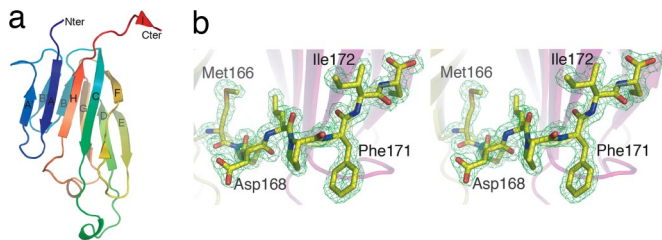


**Fig. 1.** Overall structure of mGITRL. (a) Ribbon representation of mGITRL monomer structure. The conserved  $\beta$ -strands (A–H) and the extending C-terminus arm with an extra  $\beta$ -strand (I) on the end were labeled. Note that the  $\beta$ -strand F was interrupted. (b) Stereoview of the electron density for the C-terminal arm. The electron density omit map was contoured at  $2\sigma$  levels.

In retrospect, these unexpected structural features of mGITRL explain why our attempts to determine the structure by molecular replacement failed.

**mGITRL Associates as a Dimer.** We screened for different forms of crystals by varying pH, temperature, and protein concentration to test whether mGITRL can be crystallized in a trimeric form that is consistent with the structural paradigm of the TNF/TNFR super family. However, we were unable to obtain crystals that contained mGITRL trimer. Instead of forming a trimer seen for classical TNFSF members, mGITRL forms a dimer with two subunits A and B related by  $141^\circ$  (Fig. 2*a*). The pseudo symmetry axis is perpendicular to the putative membrane orientation.

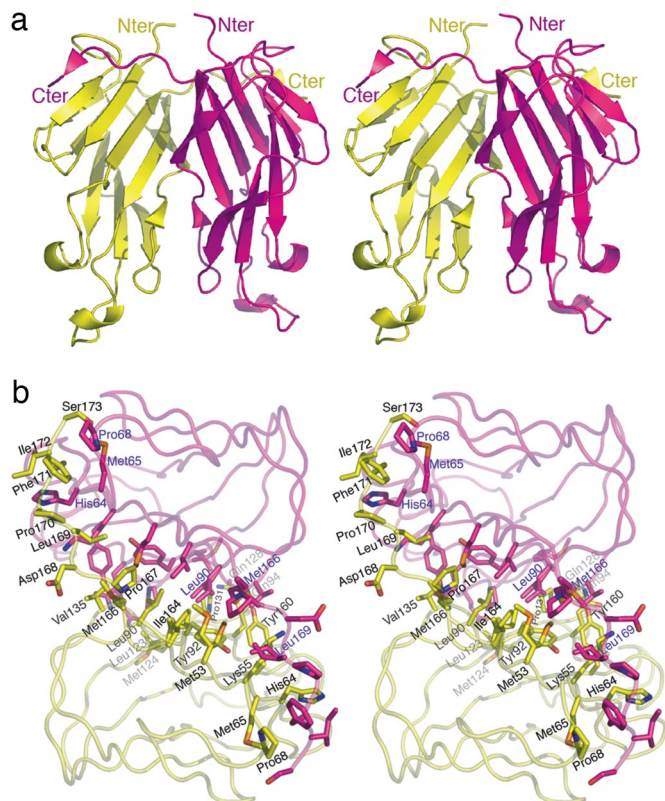


**Fig. 2.** mGITRL associates as a dimer. (a) Stereoview of mGITRL dimer. Protomers A and B are yellow and pink, respectively. The C-terminus extra  $\beta$ -strand (I) from one protomer joins the  $\beta$ -sheet (A'–A–H–C–F) of the other to form an extended intermolecular  $\beta$ -sheet (I–A'–A–H–C–F). (b) GITRL dimer interface viewed down the 2-fold axis. Residues on the dimeric interface are highlighted in the stick model. Alternative conformations for residues Ile-164 and Met-53 of protomer A and Leu-90, Met-166 and leu169 of protomer B are shown.

A salient feature of the mGITRL dimer is the intermolecular  $\beta$ -sheets formed between the extending C-terminus tethering arm of one protomer and the inner  $\beta$ -sheet (A'–A–H–C–F) of the other. Notably, the intervening loop region connecting the two discontinuous parts of the broken  $\beta$ -strand F was positioned at the interface of the dimeric core. The intermolecular  $\beta$ -sheet is stabilized by the hydrophobic packing formed between the side chains of Pro-170, Phe-171, and Ile-172 of one protomer, and those of His-64, Met-65, and Pro-68 of the other (Fig. 2*b*). The extension of the intermolecular  $\beta$ -sheets at the C terminus stabilizes the dimeric association through residues Ile-164, Met-166, Pro-167, and Leu-169 and six water molecules. The molecular surface of mGITRL is also altered to favor its dimerization. Particularly, residues Met-53, Leu-90, Tyr-92, Leu-123, Pro-131, Val-135, Tyr-160, Ile-164, Met-166, Pro-167, and Leu-169 from both protomers stabilize the dimer through extensive hydrophobic contacts at the interface. Interestingly, residues Met-53 and Ile-164 from protomer A and Leu-90, Met-166 and Leu-169 from protomer B showed dual conformations in their side chains.

The dimerization resulted in a buried molecular surface of  $\approx 3,700 \text{ \AA}^2$  with a shape complementarity ( $S_c$ ) of 0.775 between the two protomers. This observation is similar to  $\approx 4,000 \text{ \AA}^2$  for the mouse OX40L open trimer but in contrast to  $\approx 12,000 \text{ \AA}^2$  for B cell activating factor and lymphotoxin (LT). In the crystal packing analysis, hydrophobic residues Pro-170, Phe-171, and Ile-172 from the C terminus, Pro-68 from the A'B' loop, and the apolar part of Lys-69 form a small hydrophobic patch that dominates the lattice contacts. However, there was no indication for a hexameric (trimer of dimers) association.

**mGITRL Exists in Equilibrium of Dimer and Monomer in Solution.** To determine whether the dimer observed in the crystal lattice also exists in solution, we performed analytical ultracentrifugation studies, which revealed an equilibrium between the mGITRL monomers and dimers without a significant presence of trimers (Fig. 3). At  $10 \mu\text{M}$  concentration, mGITRL in solution contains approximately an equal number of monomers and dimers. At very low concentration ( $<1 \mu\text{M}$ ), monomeric form dominates the population, consistent with the observation from our gel filtration experiment. The fraction of dimers in the solution increased in a concentration-dependent manner. Combined with structural analysis, these studies suggest that the mGITRL C-terminus tethering arm might be mobile and can undergo conformational changes to favor different orders of oligomerization.

**Putative mGITR–mGITRL Complex.** Recently the LT  $\beta$  receptor (LT $\beta$ R) and LIGHT complex, also members of the TNF/TNFR super family, were shown to bind with a 2:1 stoichiometry based on biophysical studies (12). To investigate whether dimeric mGITRL and mGITR might also form 2:1 or 2:2 receptor complexes, we used the known structure of the OX40L–OX40 complex (11) for the modeling of receptor binding. Our analysis revealed that two crevices formed on the molecular surface of the mGITRL dimer may allow receptor binding (Fig. 4). The putative receptor–ligand complex model was obtained by superimposing one mGITRL protomer onto one OX40L molecule within the mOX40L–mOX40 complex. Then a dimeric mGITRL–OX40 receptor–ligand complex was modeled based on the structure of mGITRL dimer. Two OX40 receptor chains (which represent the positioning of mGITR) were positioned into the two crevices to build a hypothetical model of a 2:2 or 2:1 ligand–receptor complex (Fig. 4). The distance between the two docked receptors was  $\approx 50 \text{ \AA}$ , which is similar to that observed in the OX40L–OX40L complex. In this model, the first cysteine-rich domain of the receptor chains showed significant contacts with the C-terminal region of mGITRL. The C terminus was sandwiched by the receptor chain and the other mGITRL protomer. Thus, residues Asp-168, Pro-170, Phe-171, and Ile-172 of mGITRL may interact with the receptor molecule.

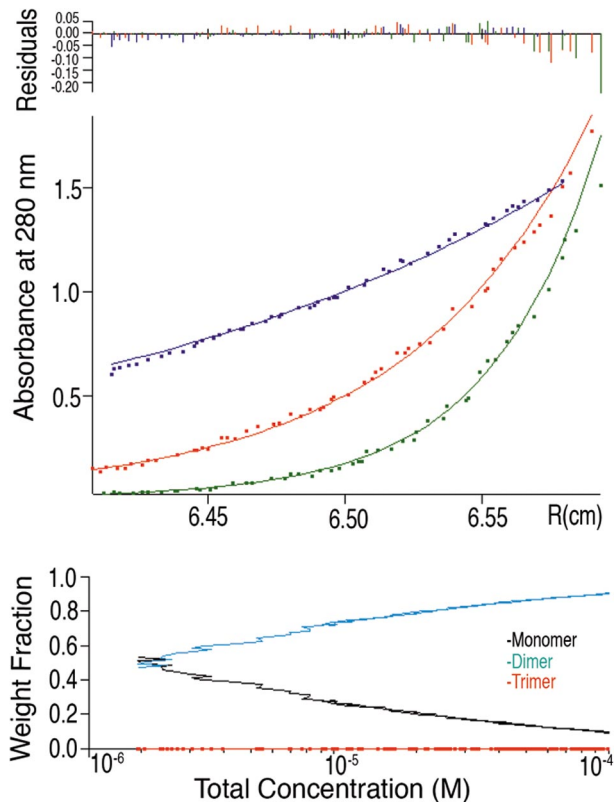


**Fig. 3.** Ultracentrifugation analysis of mGITRL. (Upper) Experimental radial concentration profiles (points) and fits (lines) to a monomer–dimer–trimer equilibrium model at three different speeds (15, 25, and 33 K RPM, respectively). (Lower) Calculated weight fractions of monomer (decreasing), dimer (increasing), and trimer (essentially zero) for concentrations covered in the experiment.

**C Terminus of mGITRL Is Critical for GITR-Mediated Function.** Sedimentation velocity analysis, and our inability to crystallize trimeric mGITRL, indicates that mGITRL dimer is a molecular species that

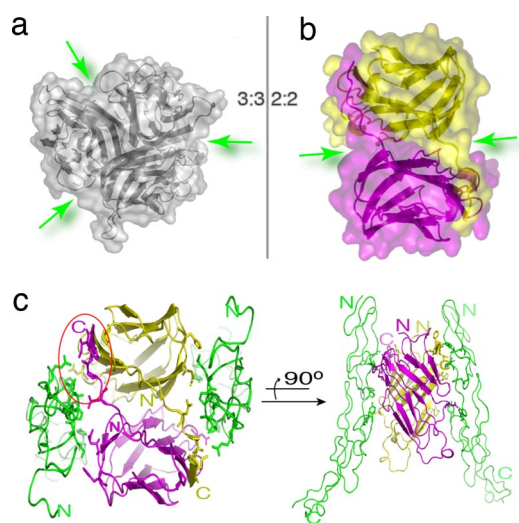


**Fig. 4.** Putative 2:2 ligand–receptor complex. (a) Molecular shape of canonical TNF trimer. Green arrow shows the putative receptor binding crevices. (b) mGITRL dimer and putative receptor binding position. (c) Model of the receptor–ligand complex based on the OX40L–OX40 complex. A model for 2:1 would be similar except one of the receptors was removed and hence is not shown.

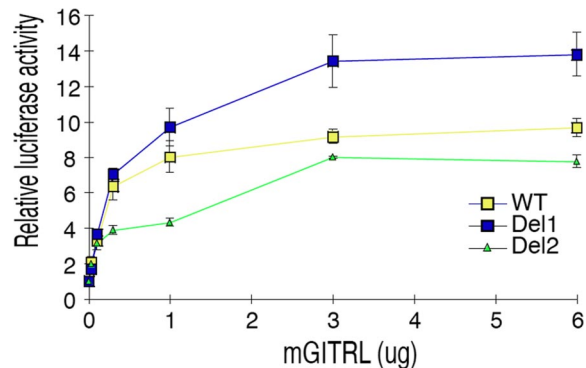


**Fig. 5.** NF- $\kappa$ B activation with wild-type mGITRL and its C-terminal deletion mutants. Cos cells were transfected with WT, mutant Del1, or mutant Del2 expression plasmids. NF- $\kappa$ B activity was measured by luciferase activity. Generated luciferase activity with each GITRL (WT, D1, or D2)/COS transfectants was compared with that generated by the COS cell transfectant with the empty vector.

may stably exist and represent a biologically relevant form. Our structural analysis also indicates that the C terminus may play a key role in mGITRL-mediated receptor activation. Earlier, we showed that the recombinant mGITRL is biologically active and able to elicit costimulatory signals through GITR (2). To investigate the contribution of the C-terminal region on signaling through GITR receptor, we generated two C-terminus deletion mutants Del1 (Phe-171–Ser-173 deleted) and Del2 (Pro-167–Ser-173 deleted). Wild-type and mutant mGITRLs at increasing levels were expressed on COS cells by transient transfection, and the ligand-mediated NF- $\kappa$ B activation was analyzed in a reporter cell (2). In this assay, a dose-dependent NF- $\kappa$ B activation was observed with the wild type and the two mutants (Fig. 5). Surprisingly, the Del1 mutant mGITRL induced higher NF- $\kappa$ B activity than that with wild-type ligand at all of the points, but the opposite was true for the mutant Del2. These observations indicate that the C terminus plays a role in receptor binding and activation.

## Discussion

GITRL and GITR are members of TNF/TNFR super family that function as costimulatory factors in the immune system. In recent years, their role in immunity has been expanded to DC and natural killer (NK) cells (13). Our studies identified a functional form of TNF family members that can activate its cognate receptor. Our structural and biological studies showed that the functionally active dimeric form is a physiologically relevant species.

Recently, the OX40–OX40L structure has been resolved (11), which shows that the ligand activates the receptor through a canonical trimeric recruitment. Comparison of mOX40L and mGITRL shows that the disposition of the C terminus differs significantly. Whereas the C terminus of mOX40L is held close to the ligand's trimer interface by a disulfide bond, mGITRL lacks this feature and has an extra stretch of three residues (Phe-171–Ile-172–Ser-173). The extra stretch forms a  $\beta$ -strand and functions as an anchor, or as a tether as observed in erbB structures (14). This C-terminus tethering arm of mGITRL is unique and important for the ligand oligomerization and receptor binding. Although dimeric form was observed in the crystal state, mGITRL exists in solution both as a monomer and dimer, and the fraction of dimers increases in a concentration-dependent manner. We reasoned that use of concentrated mGITRL protein during its crystallization might have shifted the equilibrium to favor dimer's formation. Two structural features appear to explain the apparent oligomeric switching. First, three hydrophobic residues (Pro-170, Phe-171, and Ile-172) from the C-terminus tethering arm are solvent-exposed, which in the

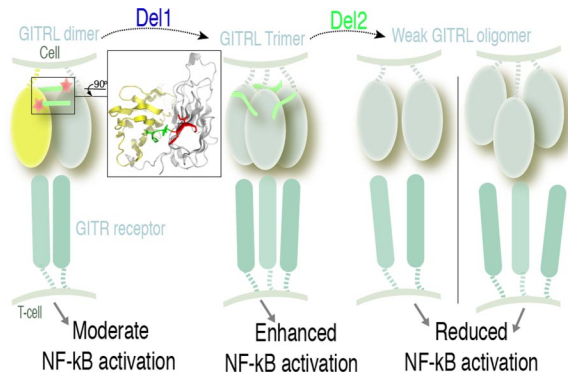


**Fig. 6.** Model for mGITRL oligomerization and signaling. mGITRL dimer stabilized by the C-terminus tether shows moderate activity, consistent with our earlier studies (15). Deletion of the anchor  $\beta$ -strand from the C-terminus tethering arm (Del1) is likely to induce conformational readjustments, so that mGITRL might form a trimer similar to OX40L. Thus, the mutant shows higher activity than that of dimer. Complete deletion of the C-terminus arm (Del2) will destabilize both dimers and trimers and therefore lead to a significant reduction in transcription activity.

absence of receptor molecules, may result in high flexibility of this region. Second, a group of residues including Met-53, Ile-163, and Ile-164 of subunit A and Leu-90, Ile-163, Met-166 and Leu-169 of subunit B exhibit alternative side-chain conformations. It is noteworthy that these residues are located on the dimeric interface and the  $\beta$ -strand H that is bent by the extending C terminus. The alternative conformations in this region suggest that there is breathing-like movement inside the dimeric core. Together, the flexible C terminus and internal breathing of mGITRL dimeric core might allow transitions between monomer and dimer, depending on the concentration.

Although our attempts to get recombinant Del1 and Del2 mutants for structural and biophysical studies failed, further structure analysis suggests that mGITRL can interconvert from dimer to trimer depending on the conformation of the C terminus. In crystals, the two protomers forming mGITRL dimer are related by  $141^\circ$ , which is closer to a trimeric disposition of  $120^\circ$  than a dimeric disposition of  $180^\circ$ . Using the OX40L structure, one can construct a plausible GITRL trimer model (SI Fig. 8) simply by reorientating the very C terminus of the mGITRL. Thus, the GITRL dimer might transform into a trimer once the conformation of the C terminus has changed. Based on our structural and mutational data, we speculate a model (Fig. 6) for mGITRL oligomerization in which the dimer is stabilized by the unique C-terminus tethering arm. Deletion of the C-terminal extra  $\beta$ -strand (Del1 mutant) removes the anchor of the tethering arm and, thus, will lead to the loss of constraints that is required to keep the particular conformation for dimerization. This loss of constraint will further induce flexibility on the dimeric interface, particularly in the breathing region. As a result, the C-terminus tethering arm may undergo readjustments to allow the formation of a trimeric ligand that might explain the Del1 mutant's enhanced activity. Moreover, according to this model, the reconfigured C terminus can be involved in trimerization similar to OX40L trimer. However, a complete deletion of C-terminus tethering arm (Del2 mutant) would decrease both the dimeric and the trimeric interactions and concomitant reduction of activity. Although the exact nature of oligomerization remains to be defined, taken together, the differences in the NF- $\kappa$ B activities of different mutants may reflect the different oligomerization states of these ligands. In the presence of receptor, mGITRL may adopt either dimeric or trimeric association via C terminus-mediated conformational changes.

Binding of mGITRL to mGITR in either 2:2 or 3:3 stoichiometry may have implications for innate and adaptive immunity. The

unique nature of GITR's role in immunity may require the ligand to exist in different oligomeric forms to elicit a controlled signaling. GITRL's ability to regulate GITR signaling as a dimer or trimer might be critical for context dependent (i.e., APC/T cell or NK cells or DC) function because abnormal expression levels of GITRL can greatly influence innate/adaptive immunity. For example, overexpression of mGITRL might lead to development of autoimmunity by more sustained activation of the immune system through activation of T effector cells (2) and simultaneous mGITRL-induced neutralization of suppressive activity of  $CD4^+CD25^+$  regulatory T cells (15). Limited expression of mGITRL might result in reduced immune reactivities because of a diminished ability to provide costimulatory signals.

Oligomerization-driven ligand-dependent receptor activation is thus far known to be mediated by trimer or trimer-of-trimer forms in the TNF/TNFR super family (16). The existence of an intermediate dimerization species has not been reported, whereas biological and regulatory activities of dimeric TNFRs have been reported (17). Our studies suggest that oligomerization intermediates involve dimers. Further studies of receptor–ligand complexes will determine whether dimeric and trimeric forms of GITRL have structural features that explain differential signaling.

## Materials and Methods

**Construction of mGITRL Expression Plasmids.** GITRL protein for crystal structural analysis was produced by the *Escherichia coli* expression system, and for functional study, GITRL protein was expressed on cell surface with a mammalian expression system. To construct the *E. coli* expression plasmids, pRSET (Invitrogen) was used as described (2). To construct the mammalian expression plasmids, pMF-neo expression vector (carrying the EF-1 $\alpha$  promoter and the neomycin-resistant gene) was used. Two mutant cDNAs encoding mutant Del1 and Del2 was generated by PCR using the mGITRL HindF primer and either the Del1 SalB (for Del1 mutant) or the Del2 SalB (for Del2 mutant) primer. These cDNAs and the wild-type GITRL cDNA were integrated into HindIII and XhoI sites of pMF neo vector. PCR primers used were: mGITRL HindF, AATAAGCTTAGCCTCATGGAGGAAATGCC; Del1 SalB, AAACGTC-GACTCTATGGTAGATCAGGCATTAAG; and Del2 SalB, AATGGTCGACCTA-CATTAAGATGATCCCCAGTATG.

**Production and Purification of GITRL Proteins Using the *E. coli* Expression System.** mGITRL protein was purified by using a *E. coli* expression system as described (2) with minor modifications. Briefly, *E. coli* BL21(DE3)pLysS was transformed with the GITRL expression plasmids. Production of the recombinant protein was induced by isopropyl  $\beta$ -D-thiogalactoside (final 1 mM) for 4 h. *E. coli* cells were lysed with BugBuster HT (Novagen) and dialyzed against Ni-NTA (Qiagen) binding buffer (50 mM  $NaH_2PO_4$ , 150 mM NaCl, pH 8.0) with 10 mM imidazole. Insoluble fraction was removed by centrifuge, and Ni-NTA was added. After 2 h of incubation, Ni-NTA was washed with binding buffer containing 20, 50, and 70 mM imidazole. The sample was then eluted with 250 mM imidazole in binding buffer, dialyzed against EKMax reaction buffer (50 mM Tris-HCl, 1 mM CaCl<sub>2</sub>, 0.1% Tween-20, pH 8.0), and digested with EKMax (Invitrogen; 1 unit per 100  $\mu$ g of protein) at  $37^\circ C$  for overnight. EKMax was removed by EK-Away resin according to the manufacturer's instruction (Invitrogen). The samples were dialyzed against Ni-NTA binding buffer with 10 mM imidazole, and His tags were removed by Ni-NTA.

**Crystallization and Data Collection.** The mGITRL was concentrated to 12 mg/ml in 20 mM Tris buffer pH 8.0 for crystallization. Single crystals were grown at  $18^\circ C$  in hanging drops containing equal volumes of sample solution and well buffer (100 mM Hepes pH 7.5 and 20% PEG 10000). Crystals appeared the next day and continued to grow to a size up to 300  $\mu$ m within a week. Heavy atom derivatives were prepared by soaking native crystals in well buffer containing an additional 5 mM  $K_2PtCl_4$  for 2 h or 1 mM  $HgCl_2$  overnight. Crystals were flash-frozen in liquid nitrogen by using the well buffer containing an additional 25% glycerol as cryoprotectant. All of the datasets were collected with our in-house Rigaku Raxis IV++ system. The observed reflections were reduced, merged, and scaled with DENZO and SCALEPACK in the HKL2000 package (18). Data processing statistics are shown in SI Table 1.

**Structure Determination and Refinement.** Multiple isomorphous replacement and anomalous scattering (MIRAS) were used to obtain phases in the Solve and Resolve packages (19, 20). About 60% of secondary structures were traceable

from the electron density maps calculated by using initial phases obtained from MIRAS. Individual fragments of the two major  $\beta$ -sheets with 28% sequence homology to EDA2 (21) were then manually fitted into the 2.5-Å electron density map, followed by rigid body refinement. Iterative cycles of model building using O (22) and refinement using CNS (23) yielded the present model, which includes residues 49–173 of mGITRL. The asymmetric unit contained two monomers (A and B). The side chains of residues Lys-104 and Lys-147 in monomer B and residues Ile-49 and Glu-50 in both monomers were disordered. All of the rest residues were well defined. Model quality was evaluated with PROCHECK (24). Refinement statistics are shown in SI Table 1. Buried surface area and complementarity was calculated by using the programs AREAIMOL and SC, respectively, from the CCP4 package (25).

**Ultracentrifuge Analysis.** Experiments were performed on a Beckman XLI analytical ultracentrifuge at 5°C. Protein was dissolved in Tris-HCl buffer at pH 7.5 and loaded into six-sector cells. Samples were centrifuged to equilibrium (no change in profile in successive 2-h scans). Data were analyzed with Igor Pro (Wavemetrics) to globally fit data at three different speeds to the equation:

$$Abs = \epsilon C_o l \exp \left[ \frac{\omega^2}{2RT} M_w (r^2 - r_o^2) \right] + \sum_{n>1}^n \epsilon n \frac{C_o^n}{K_{dn}} l \exp \left[ \frac{\omega^2}{2RT} n M_w (r^2 - r_o^2) \right] + E,$$

- Nocentini G, et al. (1997) A new member of the tumor necrosis factor/nerve growth factor receptor family inhibits T cell receptor-induced apoptosis. *Proc Natl Acad Sci USA* 94:6216–6221.
- Tone M, et al. (2003) Mouse glucocorticoid-induced tumor necrosis factor receptor ligand is costimulatory for T cells. *Proc Natl Acad Sci USA* 100:15059–15064.
- Stephens GL, et al. (2004) Engagement of glucocorticoid-induced TNFR family related receptor on effector T cells by its ligand mediates resistance to suppression by CD4+CD25+ T cells. *J Immunol* 173:5008–5020.
- Gurney AL, et al. (1999) Identification of a new member of the tumor necrosis factor family and its receptor, a human ortholog of mouse GITR. *Curr Biol* 9:215–218.
- Nocentini G, et al. (2000) Gene structure and chromosomal assignment of mouse GITR, a member of the tumor necrosis factor/nerve growth factor receptor family. *DNA Cell Biol* 19:205–217.
- Watts TH (2005) TNF/TNFR family members in costimulation of T cell responses. *Annu Rev Immunol* 23:23–68.
- Kwon B, et al. (1999) Identification of a novel activation-inducible protein of the tumor necrosis factor receptor superfamily and its ligand. *J Biol Chem* 274:6056–6061.
- Riccardi C, Cifone MG, Migliorati G (1999) Glucocorticoid hormone-induced modulation of gene expression and regulation of T-cell death: Role of GITR and GILZ, two dexamethasone-induced genes. *Cell Death Differ* 6:1182–1189.
- Zhang G (2004) Tumor necrosis factor family ligand-receptor binding. *Curr Opin Struct Biol* 14:154–160.
- Bossen C, et al. (2006) Interactions of tumor necrosis factor (TNF) and TNF receptor family members in the mouse and human. *J Biol Chem* 281:13964–13971.
- Compaan DM, Hymowitz SG (2006) The crystal structure of the costimulatory OX40–OX40L complex. *Structure (London)* 14:1321–1330.
- Eldredge J, et al. (2006) Stoichiometry of LTbetaR binding to LIGHT. *Biochemistry* 45:10117–10128.
- Nocentini G, Ronchetti S, Cuzzocrea S, Riccardi C (2007) GITR/GITRL: More than an effector T cell costimulatory system. *Eur J Immunol* 37:1165–1169.
- Ward CW, Lawrence MC, Streltsov VA, Adams TE, McKern NM (2007) The insulin and EGF receptor structures: New insights into ligand-induced receptor activation. *Trends Biochem Sci* 32:129–137.
- Shimizu J, Yamazaki S, Takahashi T, Ishida Y, Sakaguchi S (2002) Stimulation of CD25(+)CD4(+) regulatory T cells through GITR breaks immunological self-tolerance. *Nat Immunol* 3:135–142.
- Cachero TG, et al. (2006) Formation of virus-like clusters is an intrinsic property of the tumor necrosis factor family member BAFF (B cell activating factor). *Biochemistry* 45:2006–2013.
- Bazzoni F, Alejos E, Beutler B (1995) Chimeric tumor necrosis factor receptors with constitutive signaling activity. *Proc Natl Acad Sci USA* 92:5376–5380.
- Otwinowski Z, Minor W (1997) Processing of x-ray diffraction data collected in oscillation mode. *Methods Enzymol* 276:307–326.
- Terwilliger TC (2003) Automated main-chain model building by template matching and iterative fragment extension. *Acta Crystallogr D* 59:38–44.
- Terwilliger TC, Berendzen J (1999) Automated MAD, MIR structure solution. *Acta Crystallogr D* 55:849–861.
- Hymowitz SG, et al. (2003) The crystal structures of EDA-A1 and EDA-A2: splice variants with distinct receptor specificity. *Structure (London)* 11:1513–1520.
- Jones TA, Zou JY, Cowan SW, Kjeldgaard M (1991) Improved methods for building protein models in electron density maps and the location of errors in these models. *Acta Crystallogr A* 47:110–119.
- Brunger AT, et al. (1998) Crystallography and NMR system: A new software suite for macromolecular structure determination. *Acta Crystallogr D* 54:905–921.
- Laskowski RA, MacArthur MW, Moss DS, Thornton JM (1993) PROCHECK: A program to check the stereochemical quality of protein structures. *J Appl Crystallogr* 26:283–291.
- CCP4 (1994) The CCP4 suite: Programs for protein crystallography. *Acta Crystallogr D* 50:760–763.

where  $c_o$  is the concentration of monomer at  $r_o$ ,  $\epsilon$  is the molar extinction coefficient,  $l$  is the optical path length,  $\omega = 2\pi \times \text{RPM}$ ,  $R = 8.3144\text{E7 erg } ^\circ\text{K}^{-1}\text{mol}^{-1}$ ,  $T$  is the temperature in  $^\circ\text{K}$ ,  $M_w$  is the monomer molecular weight,  $K_{dn}$  is the monomer- $n$ mer dissociation constant, and  $E$  is baseline (zero concentration) absorbance. The summation is over all  $n$ -mer states above monomer considered in the equilibrium. In this work, we used two terms in the summation representing a three-state monomer–dimer–trimer equilibrium ( $n = 2, 3$ ). The contribution of the trimer however, was, found to be negligible.

**NF- $\kappa$ B Luciferase Reporter Assay.** Cos cells ( $2 \times 10^6$ ) were transfected with wild-type, Del1, or Del2 mutant GITRL expression plasmid (0.03, 0.1, 0.3, 1, 3, or 6  $\mu\text{g}$ ) by Gene Pulser Xcell (BioRad) and cultured for 48 h. Cells were then treated with mitomycin C. Total DNA amount was adjusted to 6  $\mu\text{g}$  with the empty expression vector. GITR/JE6.1 transfectant cells (2) (expressing GITR on cell surface) were transfected with the NF- $\kappa$ B luciferase reporter plasmid (Stratagene) ( $1 \times 10^7$  cells with the 10- $\mu\text{g}$  reporter plasmid) by Gene Pulser Xcell and pooled, and  $5 \times 10^6$  cells were added to the Cos cell culture. After 48 h, cells were harvested, and luciferase activity was analyzed. This assay was repeated more than three times.

**ACKNOWLEDGMENTS.** We thank Dr. Yongwon Choi of the University of Pennsylvania and Susan Lea of Oxford University for their helpful suggestions, Prof. Mark L. Tykocinski of the University of Pennsylvania for support and encouragement, and Dr. Jaelyn Freudenberg for her review of the manuscript. This work was supported in part by grants from the National Institutes of Health and the National Cancer Institute (to M.I.G. and R.M.) and the Abramson Family Cancer Research Institute (to M.I.G.).